

SECURITY (

AD-A206 539 DOCUMENTATION PAGE

1a. REPORT U		1b. RESTRICTIVE MARKINGS	
3. SECURITY CLASSIFICATION AUTHORITY		3. DISTRIBUTION/AVAILABILITY OF REPORT approved for public release; distribution is unlimited	
2b. DECLASSIFICATION/DOWNGRADING SCHEDULE		5. MONITORING ORGANIZATION REPORT NUMBER(S) AFOSR-TR-89-U386	
4. PERFORMING ORGANIZATION REPORT NUMBER(S)		7a. NAME OF MONITORING ORGANIZATION AFOSR	
6a. NAME OF PERFORMING ORGANIZATION Graduate Aeronautical Labs California Institute of Technology	6b. OFFICE SYMBOL (if applicable) NA	7b. ADDRESS (City, State, and ZIP Code) Building 410 Bolling Air Force Base Washington, D.C. 20332-6448	
6c. ADDRESS (City, State, and ZIP Code) 1201 E. California Blvd. Pasadena, CA 91125	9. PROCUREMENT INSTRUMENT IDENTIFICATION NUMBER F49620-86-C-0134		
8a. NAME OF FUNDING/SPONSORING ORGANIZATION AFOSR	8b. OFFICE SYMBOL (if applicable) NA	10. SOURCE OF FUNDING NUMBERS	
8c. ADDRESS (City, State, and ZIP Code) Building 410 Bolling Air Force Base Washington, D.C. 20332-6448		PROGRAM ELEMENT NO. 61102F	PROJECT NO. 3484
11. TITLE (Include Security Classification) Unsteady and Separated Flow		TASK NO. A1	WORK UNIT ACCESSION NO.
12. PERSONAL AUTHOR(S) P.E. Dimotakis, A. Leonard and A. Roshko			
13a. TYPE OF REPORT annual technical	13b. TIME COVERED FROM 10/1/87 TO 9-30-88	14. DATE OF REPORT (Year, Month, Day) 1988, 11, 30	15. PAGE COUNT 21
16. SUPPLEMENTARY NOTATION			
17. COSATI CODES		18. SUBJECT TERMS (Continue on reverse if necessary and identify by block number)	
FIELD	GROUP	SUB-GROUP	
		Unsteady flow; separated flow, vortex interaction; flow control. (mgm) ←	
19. ABSTRACT (Continue on reverse if necessary and identify by block number)			
<p>A computer controlled system for the X-Y carriage on the Tow Tank has been installed. A force balance for measuring dynamic forces on models carried by the carriage has been built and installed. Initial measurements of such forces have been obtained on a flat-plate airfoil at various angles of attack.</p> <p>Optical and computer components have been assembled and integrated into a system for acquiring and processing streakline images of fluorescent particles in flow fields in water.</p> <p>Water-tunnel experiments on a Liebeck airfoil showed that a large cavity on the upper surface (to establish a free shear layer along the pressure plateau) promotes reattachment into the adverse pressure gradient and delays stall.</p> <p>Flow visualization and wake measurements downstream of a circular cylinder executing forced rotary oscillations showed that strong open-loop control could be exercised on</p>			
20. DISTRIBUTION/AVAILABILITY OF ABSTRACT <input checked="" type="checkbox"/> UNCLASSIFIED/UNLIMITED <input type="checkbox"/> SAME AS RPT. <input type="checkbox"/> DTIC USERS		21. ABSTRACT SECURITY CLASSIFICATION Unclassified	
22a. NAME OF RESPONSIBLE INDIVIDUAL James M McMichael		22b. TELEPHONE (Include Area Code) (202) 767-4936	22c. OFFICE SYMBOL AFOSR/NA

DC FORM 1473, 84 MAR

83 APR edition may be used until exhausted.

All other editions are obsolete.

SECURITY CLASSIFICATION OF THIS PAGE

89 4 221054 UNCLASSIFIED

ous for analyzing
ly steady but have
ys which are *intrin-*
Our approach is by
A large part of the
laboratory experiments

f the three principal **Codes**

Dist	Avail and/or Special
A-1	

software is used to generate real time incremental position commands for the Galiel board; the program was designed to generate complex (unsteady) carriage motion profiles in a user friendly manner. Some final adjustment of the control system parameters is still required to optimize carriage response vs. vibration level. This is of immediate concern for force measurements since the very slight vibration induced by the position control system is apparent in the force output traces.

Load Cell Force Balance:

This system consists of three components: the force balance itself, which is designed to be suspended below the X-Y carriage and will measure 3 force components (lift, drag and moment in a horizontal plane, a four channel amplifier/analog noise filter; and an RC-electronics computerscope data acquisition system running on an AT compatible computer. Output data are analyzed and optimally filtered using software which can output either forces or force coefficients vs. time and/or position. Amplifier gain can be adjusted to allow full scale forces of $\pm 20\text{N}$ to $\pm .02\text{N}$, the amplifier noise being about $.002\text{N}$. A 4th order low pass 25 Hz. filter is used to analog filter the signal before it is digitized to eliminate aliasing in any subsequent digital or Fourier filtering.

The balance was designed to have a *minimum* natural frequency of 25 Hz., but initial force measurements indicated the very slight vibration of the carriage due to the computer control system induced a vibration somewhere in the balance system of about 8 Hz. This resulted in a signal to noise ratio of about 2. A little further work should eliminate this vibration and a signal to noise of 30+ should be achievable.

Preliminary force measurements have been made on a specially constructed flat plate set at different angles of attack, using different acceleration profiles (both linear and sinusoidal) and at different Reynolds numbers. Zero-acceleration profiles (i.e., globally steady motion) were also investigated. In the latter case, with the flat plate at angle of attack 90° , drag histories such as that shown in Figure 3 were obtained. Although the nearly steady-state part of the history is at $C_d = 2$, close to the nominal value for flat-plate drag, there are some puzzling features, for example the early onset ($x/c = 3$) of this "steady" state, as well as the not quite steadiness (before termination at $x/c = 23$). Comparison with our numerical computations are discussed in the following section C.

(b) Investigations in Wind and Water Tunnels

The earlier steady state experiments in tow tank and wind tunnel on a flat plate with vortex "trapped" ahead of an upper flap (the Hurley-Tanveer-Saffman configuration) (Figure 4 and 5) showed that the full theoretical lift cannot be achieved because the flow separates from the upper flap soon after reattaching to its leading edge (due to the adverse pressure gradient on the upper surface of the upper flap). Various combinations of plate lengths, angle between plates, and angle of attack were investigated, as well as addition of curvature to the upper plate. Some combinations of parameters showed lift coefficients as high as 2.2 at large angles of attack ($\alpha = 40^\circ$), even with large separation. It was thought that by properly designing the upper plate, using techniques suggested by Stratford, the recovery on the upper plate could be enhanced. This led to the idea of using a Liebeck airfoil (which is designed to recover upper surface pressure) with a large cutout on that part of the upper surface which is at constant C_p (corresponding to the free streamline in the Hurley-Tanveer-Saffman model). We hoped that the cavity's free-shear-layer oscillation would provide the strong vortices necessary to

energize the boundary layer ahead of the adverse pressure gradient region, as a past experiment by Gharib has shown.

We selected and constructed a Liebeck airfoil that shows the highest theoretical lift coefficient available ($CL = 8$) in the Liebeck airfoil series. Tests were conducted on a large (1.5 ft chord length and 4 ft span) model in a water tunnel at the University of Southern California, San Diego. Initial flow visualization studies indicate that the presence of the cavity improves the reattachment length (Figure 5). The extent of the reattachment region is a strong function of flow condition in the cavity. A variety of cavity widths were tested for the optimum and non-optimum angles of attack. It was concluded that the condition of self-sustained oscillations in the cavity is very effective in extending the reattachment region, but depends strongly on the angle of attack. The optimum angle of attack for the selected Liebeck airfoil has a narrow range. As a consequence, a new Liebeck airfoil (LA 505 series), with milder adverse pressure gradient and broader range of angle of attack for optimum lift, has been designed. It also became clear that measurement of lift and drag is important for evaluating such configurations; consequently a force balance for these experiments has been designed and will be built (with UCSD funds). The Liebeck airfoils and the force balance are designed to be compatible with both the UCSD water tunnel and the GALCIT Merrill Wind Tunnel.

Work is still needed to improve the quality and quantity of the output traces.

Particle Tracing (Streakline) Flow Visualization System:

The particle tracing system consists of an American Laser Corporation 8W Argon-Ion laser whose intensity is controlled using a Bragg cell. The laser beam is split into a sheet and is used to illuminate fluorescent tracer particles in the flow; output traces are then recorded with an integrating CID camera. The time of intergration and the pulsation of the laser beam through the Bragg cell is controlled using a two channel programmable function generator which is controlled by an XT compatible computer. Final video images are digitized using a PCVision image capture board operating in an AT compatible computer; analysis software is then used to enhance the video image and calculate velocity and vorticity fields.

Work is still needed to improve the quality and quantity of the output traces. The system in its present form uses a cylindrical lens to create a sheet of laser light. Since the trace particles fluoresce more efficiently at higher incident light levels, using a scanning mirror to create the sheet should improve the sharpness of the particle streaks; the particles would then be "hit" with the full laser power in pulses, instead of a lower level steady lighting. Some development work will be required for the technique to be useful on unsteady or "complex" flows (i.e., a flow field with many small structures present) since most of its previous development has been with steady flows where the magnitude of the velocity is relatively constant and the particle density can be fairly low.

B. Feedback Control of Separated Flows

1. Research Objectives

The objective of this research is to apply feedback control to separated shear flows. Due to the very high order and nonlinear nature of this control problem, our approach will be to use an "adaptive" control method. We plan to integrate simplified equations of motion for the flow system in real time.

These equations can be thought of as the system "model". Parameters for this system will be adjusted in response to control inputs, real-time flow measurements, and by direct integration. For example, if a vortex-dynamics calculation were used, the parameters would be the locations and strengths of the vortices. The feedback loop will be closed by continuously trying to decrease a function such as the energy in the wake (a candidate Liapunov function) with respect to possible control inputs. Initially, the combined flow and controller will be simulated without the actual flow, to determine the effectiveness of this approach.

2. Status of Research

Exploratory open loop experiments have been performed on smooth circular cylinders in steady uniform flow, executing forced rotary oscillations. Our flow visualization and wake profile measurements at Reynolds numbers in the vicinity of 16,000 have shown that it is possible to produce dramatic effects on the structure of the cylinder wake by such means. In particular, a factor of five decrease in the resulting displacement thickness and estimated cylinder drag was achieved, depending on the frequency and amplitude of oscillation.

The cylinder was rotated sinusoidally at a forced Strouhal number (S_f) of $fd/U_{free-stream}$, where f = forcing frequency, d = cylinder diameter, and $U_{free-stream}$ = free stream velocity, while the peak circumferential velocity (v_{max}) was fixed at $2U_{free-stream}$. This value of v_{max} was chosen because it is greater than the maximum flow velocity in the vicinity of the unforced cylinder. As such, we expected that at the peak of the oscillation cycle, only one sign of vorticity would be created on the cylinder surface. The wake mean velocity and rms profiles reported in Figure 6 were measured four diameters downstream of the cylinder. Of particular interest is the coincidence of observations in the neighborhood of $S_f \sim 0.9$. Here we found minima for the drag coefficient (C_D) and the displacement thickness (δ/d), a transition from forcing of the wake vortices to forcing of shear layer vortices, and the ratio of vertical to horizontal vortex spacing (σ) was of order one, transitioning from $\sigma < 1$ to $\sigma > 1$ with increasing S_f .

It was observed over the entire range of observation ($0 < S_f < 2.5$) that the vortex shedding was synchronized with the forcing frequency. Visually, the wake structure took on three basic personalities. When $S_f \ll 0.2$ it was observed that the flow in the vicinity of the cylinder can look somewhat like the potential flow around a cylinder with circulation. In this region, the flow was characterized by the cylinder swinging the flow back and forth via the Magnus effect. Large vortices of alternating sign were shed between the positive and negative parts of the forcing cycle. As S_f increases past $S_f = 0.2$, the method of flow actuation changed, vorticity was collected on the low-speed side of the cylinder, while being released on the high-speed side. Here the "Magnus effect" was not apparent, and the flow around the cylinder was characterized by the shed vortices. The resulting patterns of alternating vortices persisted far downstream of the cylinder for $S_f < 0.8$. In contrast, for $S_f > 0.9$, only the shear layers separating from the cylinder were forced; these two rows of shear layer vortices were drawn toward each other, nearly closing the wake. They disintegrated upon meeting, with the wake transitioning at a lower frequency soon afterward.

The displacement thickness and drag coefficient estimates summarized in Figure 7 were calculated from the mean velocity profiles in Figure 6. Note the broad minima in C_D and δ/d around $S_f = 0.9$. There may also be one or more local minima below $S_f = 0.3$, but this possibility was not investigated.

The validity of the estimated C_D below $S_f \sim 0.2$ is in question because of the large velocity fluctuations. We suspect that C_D has been underestimated in that region. The error bars in Figure 7b reflect the uncertainty due to the velocity fluctuations.

These open loop experiments suggest that control of bluff body flows can be accomplished by encouraging the inevitable (alternating) vortices to occur at a specified strength and rate, using the subsequent vortex interactions to control the wake.

C. Numerical Simulation of Separated Flows

1. Research Objectives

This work has aimed to perform, using vortex methods, two- and three-dimensional numerical simulations of the dynamics of large-scale separated vortices in the near wake of a bluff body and to study the mutual interactions between the vortex structures and the body during transient motions. A primary objective in this part of the research is to complement and interact strongly with the experimental parts of the research. Our objectives for the development of the required computational tools suitable computational elements and dynamical equations. include the following capabilities:

- (a) Represent the vortex dynamics in the near and far wake using suitable computational elements and dynamical equations.
- (b) Satisfy the inviscid boundary condition at the solid surface, i.e., no flow through the walls, and
- (c) Determine the locations of the separation points in time, the flux of vorticity into the outer flow and, if necessary, faithfully represent the state of the boundary layer in the vicinity of reattachment.

2. Status of Research

(a) To represent the vortex dynamics in the near and far wake of a three-dimensional separated flow, we have developed a robust three-dimensional vortex method using vector-valued vortex particles. These vectors move with the local velocity and stretch and rotate in response to the local strain rate. A major problem that was encountered was the treatment of dissipation. Without some form of dissipation or subgrid scale modeling, vortex calculations, which attempt to satisfy the inviscid equations of motion, typically produce singularities in finite time that terminate the simulation. We have derived a nonlinear viscous model for vortex simulations that is related to the Smagorinsky model for grid-based large-eddy simulations. The method was tested successfully on two separate problems involving the interaction of two vortex rings. Several notable phenomena were observed during these interactions: (1) complex motions of the space curves of the vortex tubes, (2) development of internal structure (other than swirling flow) such as axial flows and vortex breakdown, and (3) reconnection of vortex lines.

(b) In the numerical simulation of unsteady and separated flows of interest we use vortex panels to represent the boundary-layer vorticity. The usual formulation for the panel method on a flat plate leads to a singularity. Recently, we have derived a new algorithm to determine the local boundary layer

circulation per unit area on either side of a flat plate given an arbitrary wake vorticity distribution. This allows us to construct boundary-layer separation models that have a firm physical basis. We are now testing the new scheme on a variety of two-dimensional flows past a flat plate including oscillations in angle of attack with very encouraging results. In some cases (e.g., drag of a flat plate at 90° angle of attack) the aerodynamic forces are higher than those measured in various experiments including the present ones. Clearly more understanding and refinement of the experiments and the computations are needed. We are planning further computations and tow-tank experiments to determine if the discrepancy is due to a modeling or numerical problem in the computation or three-dimensional effects in the experiments.

(c) As a first application of our computational tools developed for two-dimensional flows, we investigated flow past a flat plate for a fixed 90° angle of attack and for sinusoidal oscillations in angle of attack about 90° . For a flat plate held at a constant $\alpha = 90^\circ$ we obtained the time-dependent drag coefficient (C_D) shown in Figure 8. During the first 25 units of time, i.e., $x/c = 25$ ($U_\infty = 1$ and plate length $L = 1$) the flow is unsteady but nearly symmetric about the horizontal axis (see Figure 9) and C_D drops below 1.0, consistent with free-streamline theory. However, for $t > 30$, the flow becomes highly asymmetric and evolves into the expected, nearly periodic vortex shedding mode. The average drag is high ($\langle C_D \rangle \sim 3.6$) as a strong vortex is formed near each end of the plate (Figure 10) and remains there for a substantial fraction of each half-cycle, resulting in a high average suction distribution on the backside of the plate.

Inspired by cylinder wake control experiments performed in the experimental part of the research, in which rotary oscillations of the cylinder dramatically reduced the drag, we investigated the effect of angle of attack oscillations on the drag of a flat plate with an average angle of attack of 90° . Using an oscillation frequency of about five times the natural shedding frequency and a maximum tip speed of 2.0, we found a significant drop in the average drag to $\langle C_D \rangle \approx 2.3$ (Figure 11) along with significant change in the flow structure. Under the new conditions with oscillations, two vortices are formed at each end of the plate during each half cycle. The two vortices have opposite sign circulation and therefore induce each other to move away from the plate (Figure 12) so that the suction on the backside of the plate is reduced.

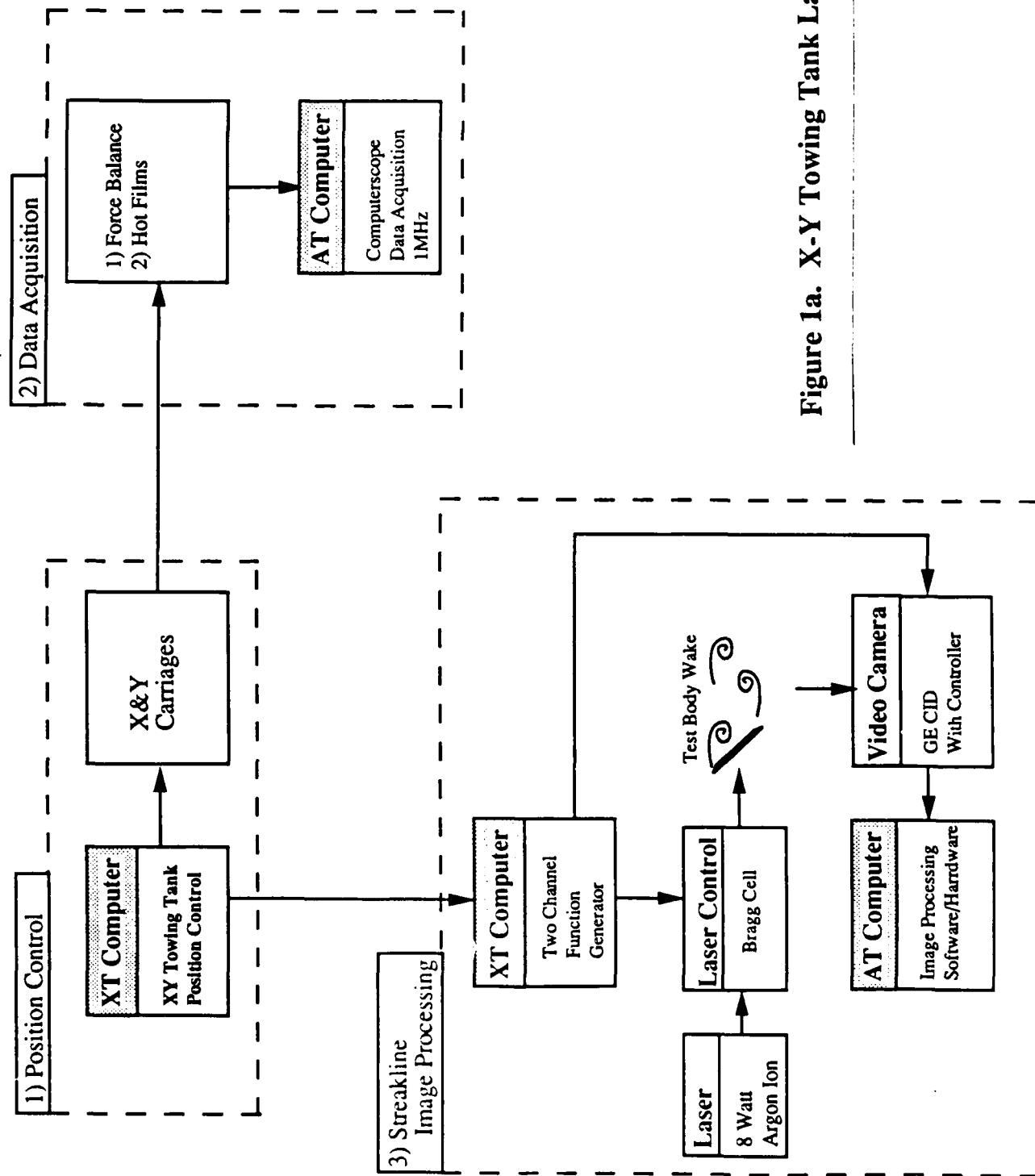


Figure 1a. X-Y Towing Tank Lab Layout

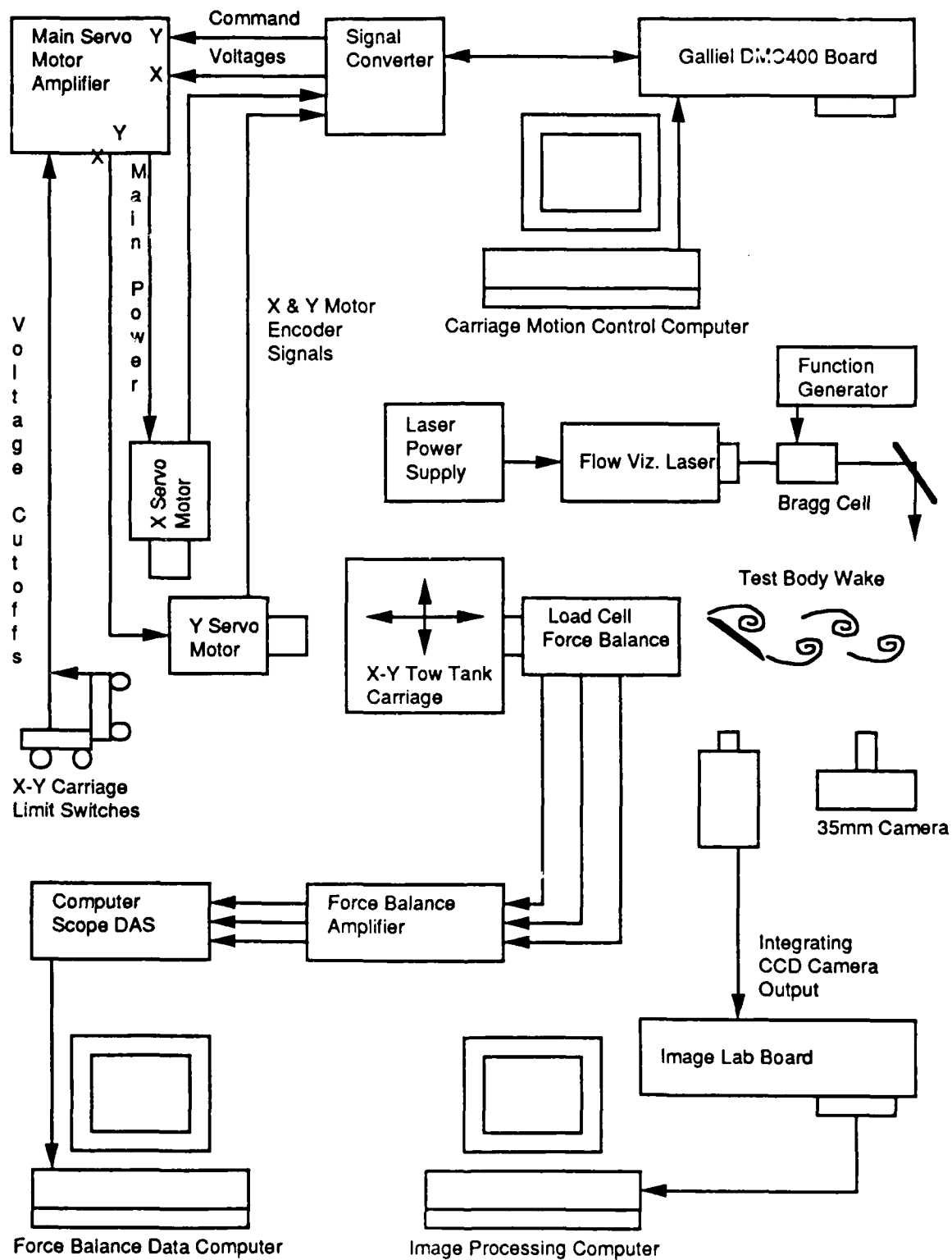


Figure 1b. X-Y Towing Tank Lab Layout

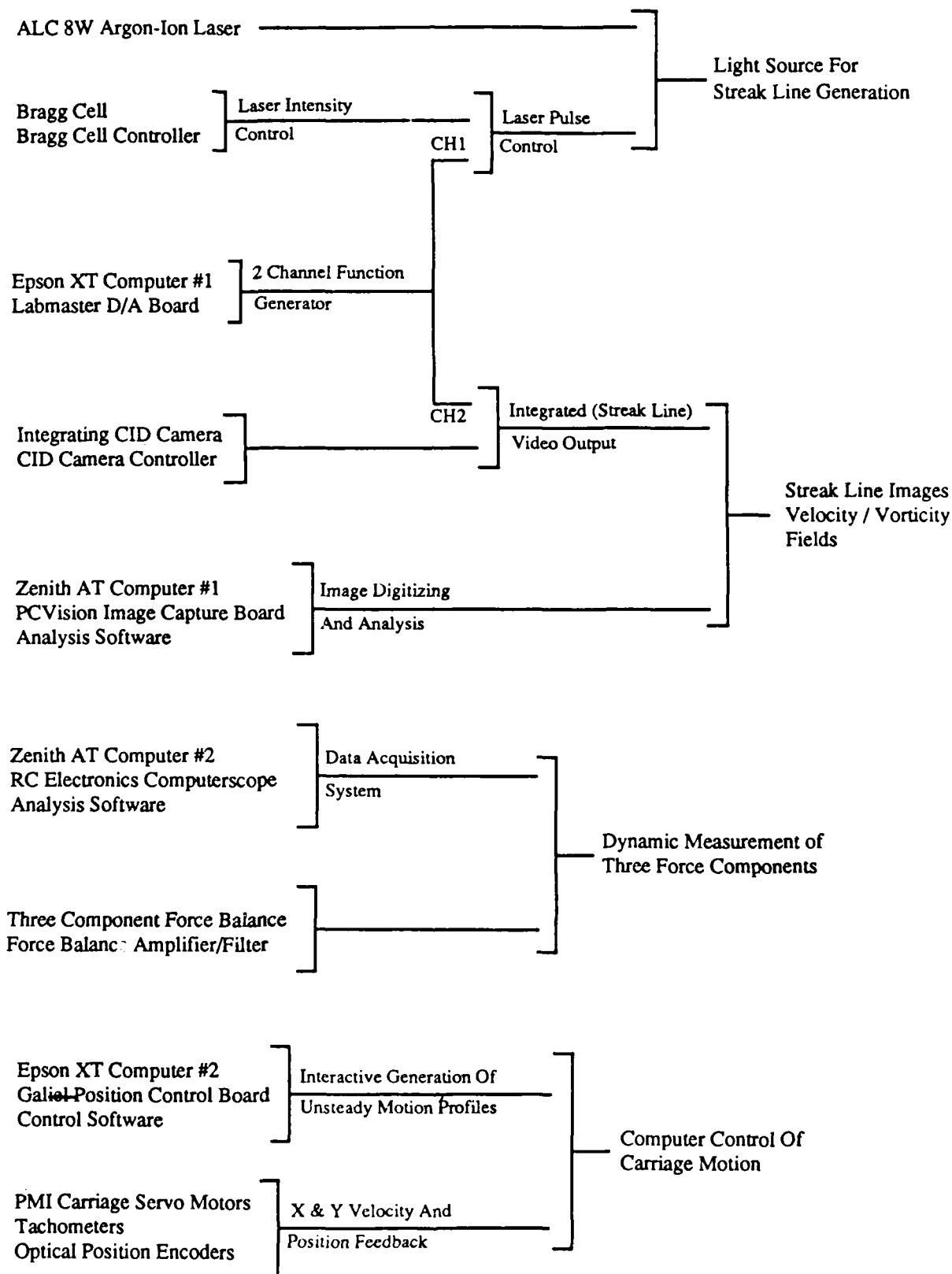


Figure 2. X-Y Towing Tank Equipment Organization

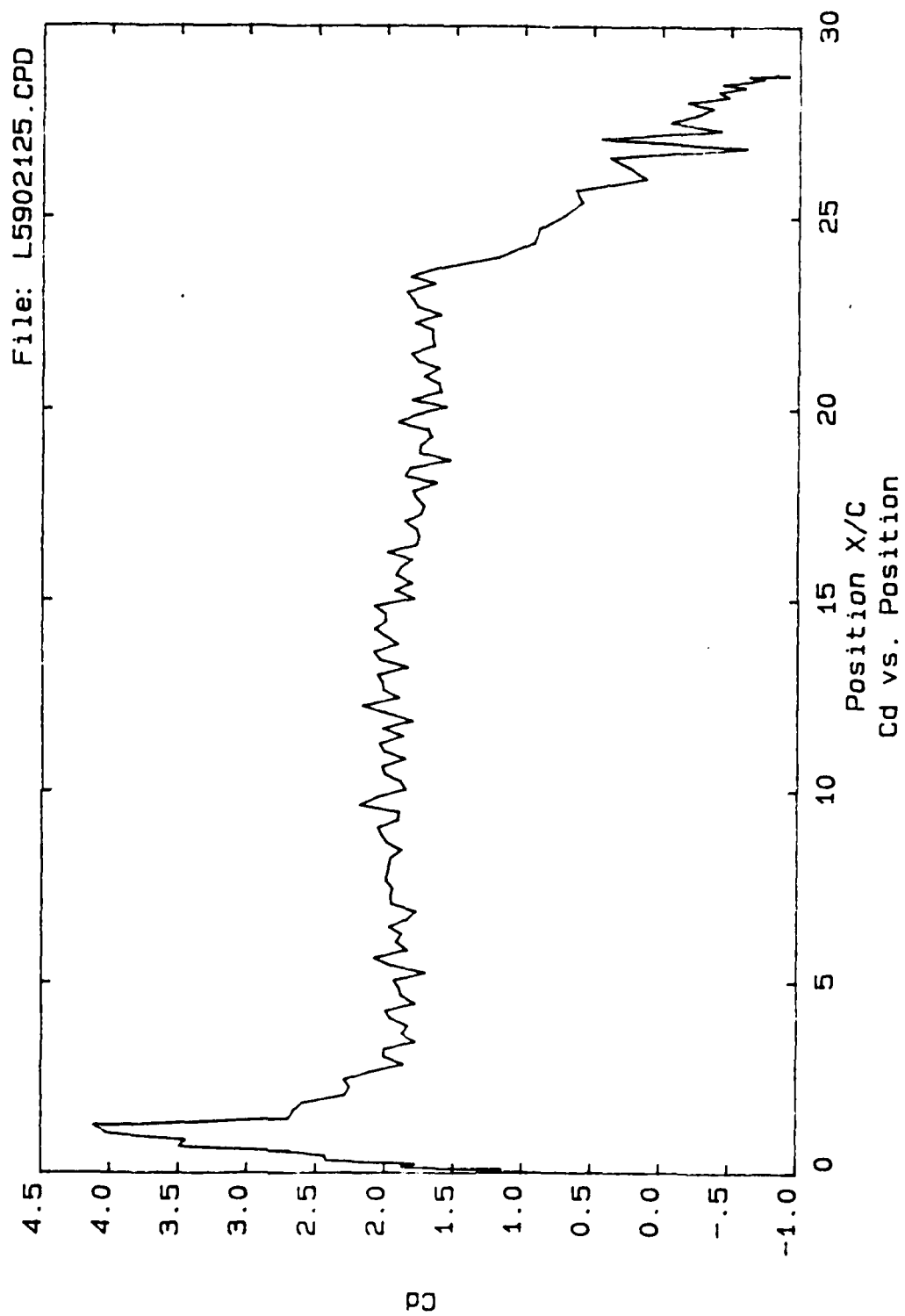
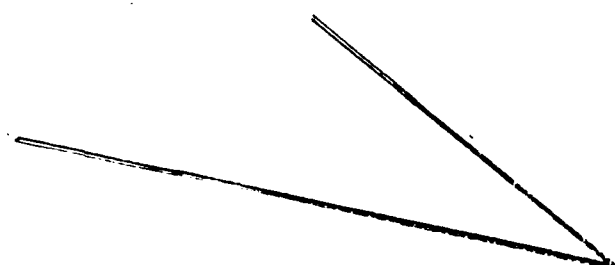


Figure 3. C_D vs x/c



- (i) Flat plate with upper flap (Hurley-Saffman-Tanveer configuration).

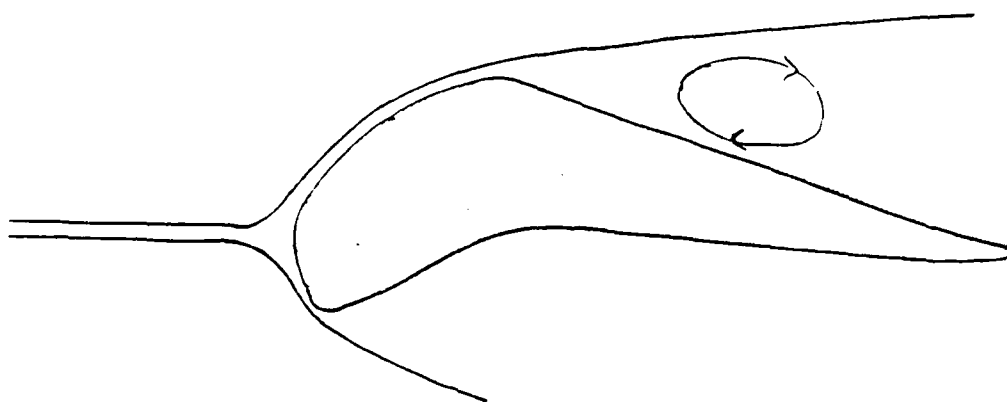


- (ii) Flat plate with curved upper flap.



- (iii) Both plates curved (Liebeck airfoil with gap).

Figure 4. Evolution of Airfoil Configurations



Liebeck airfoil without cavity

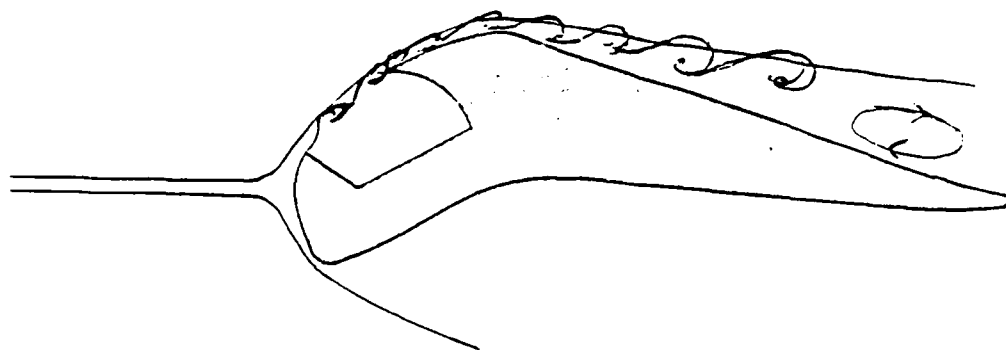


Figure 5. Liebeck Airfoil with Cavity

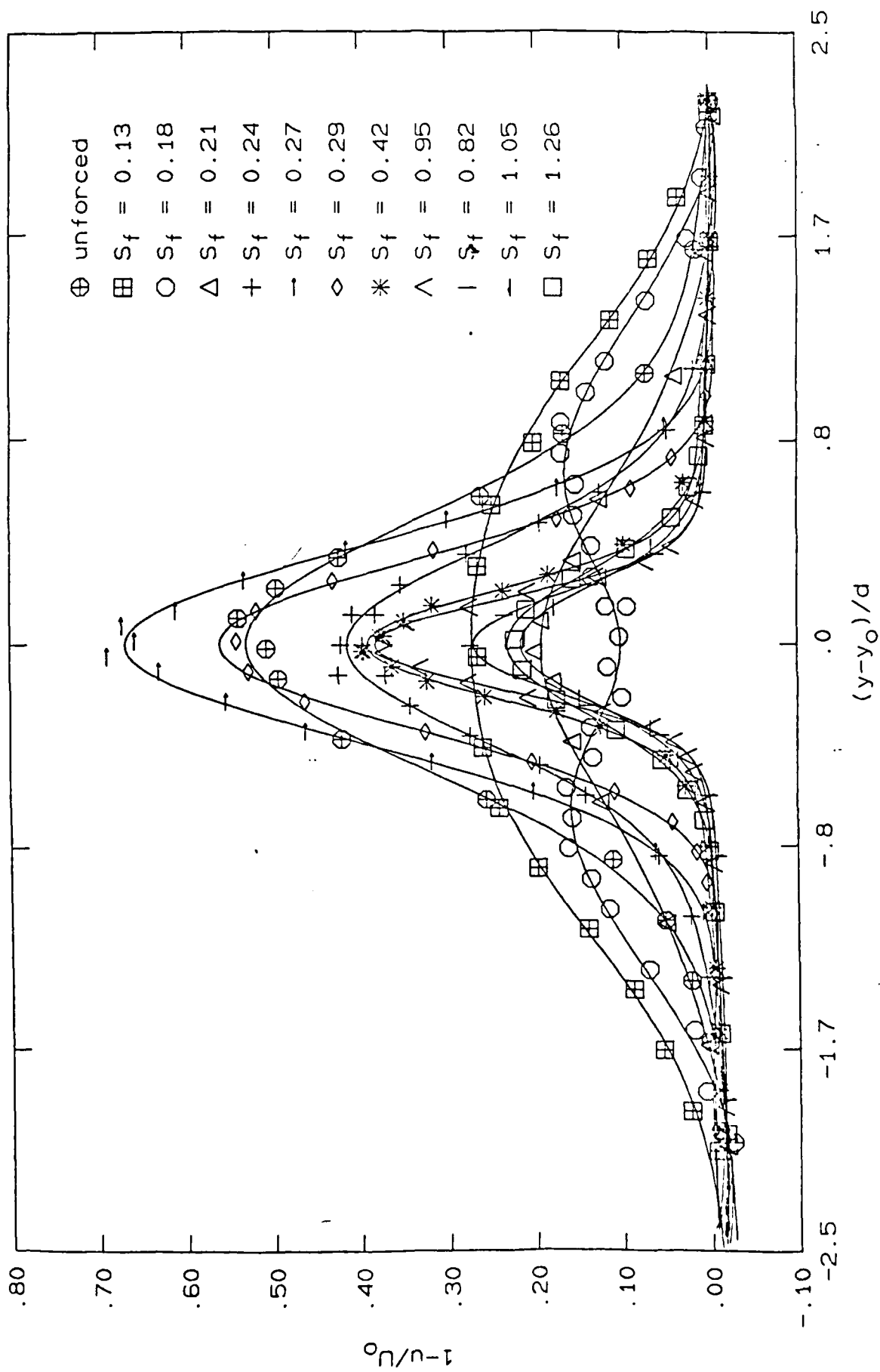
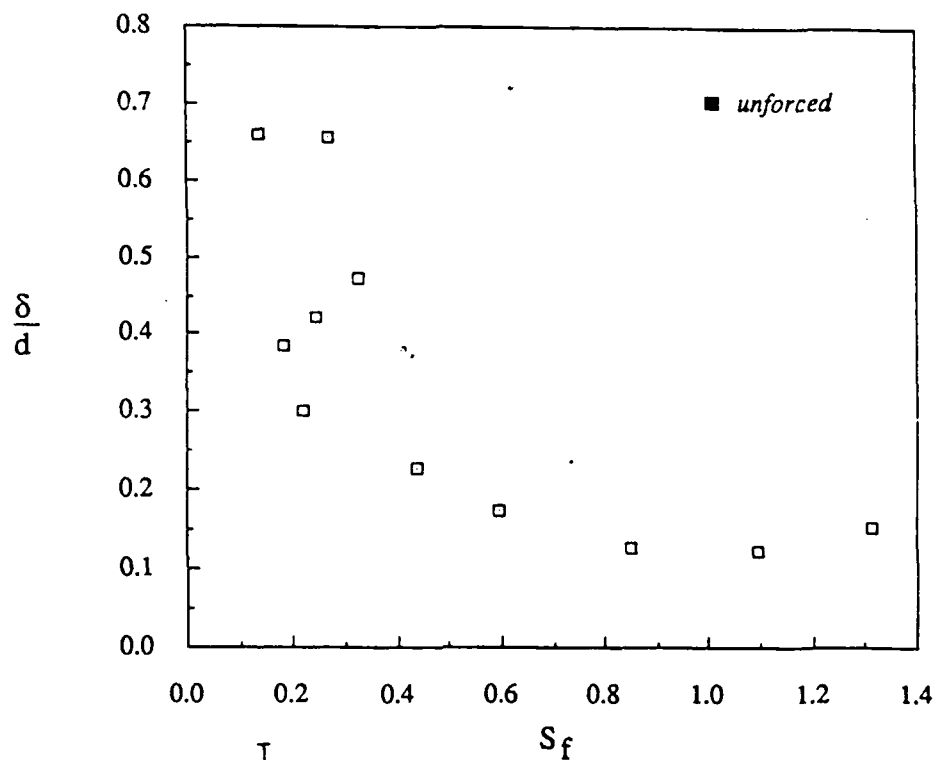
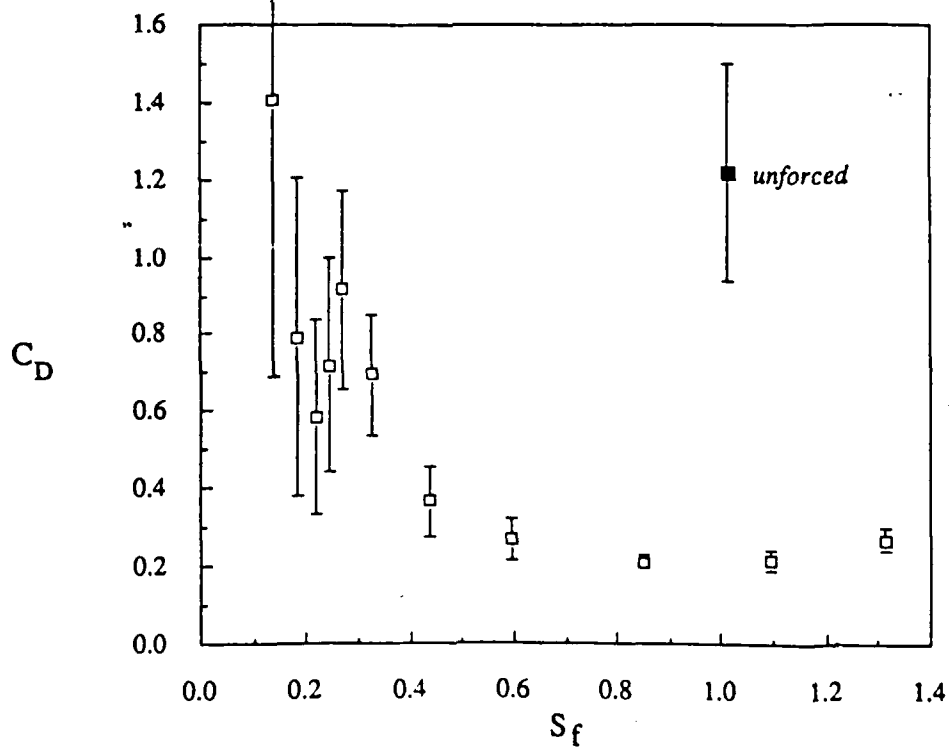


Figure 6. Mean Velocity Profiles at $x/d = 4.0$



(a) variation of displacement thickness with forcing frequency



(b) variation of drag coefficient with forcing frequency

Figure 7. δ/d and C_D

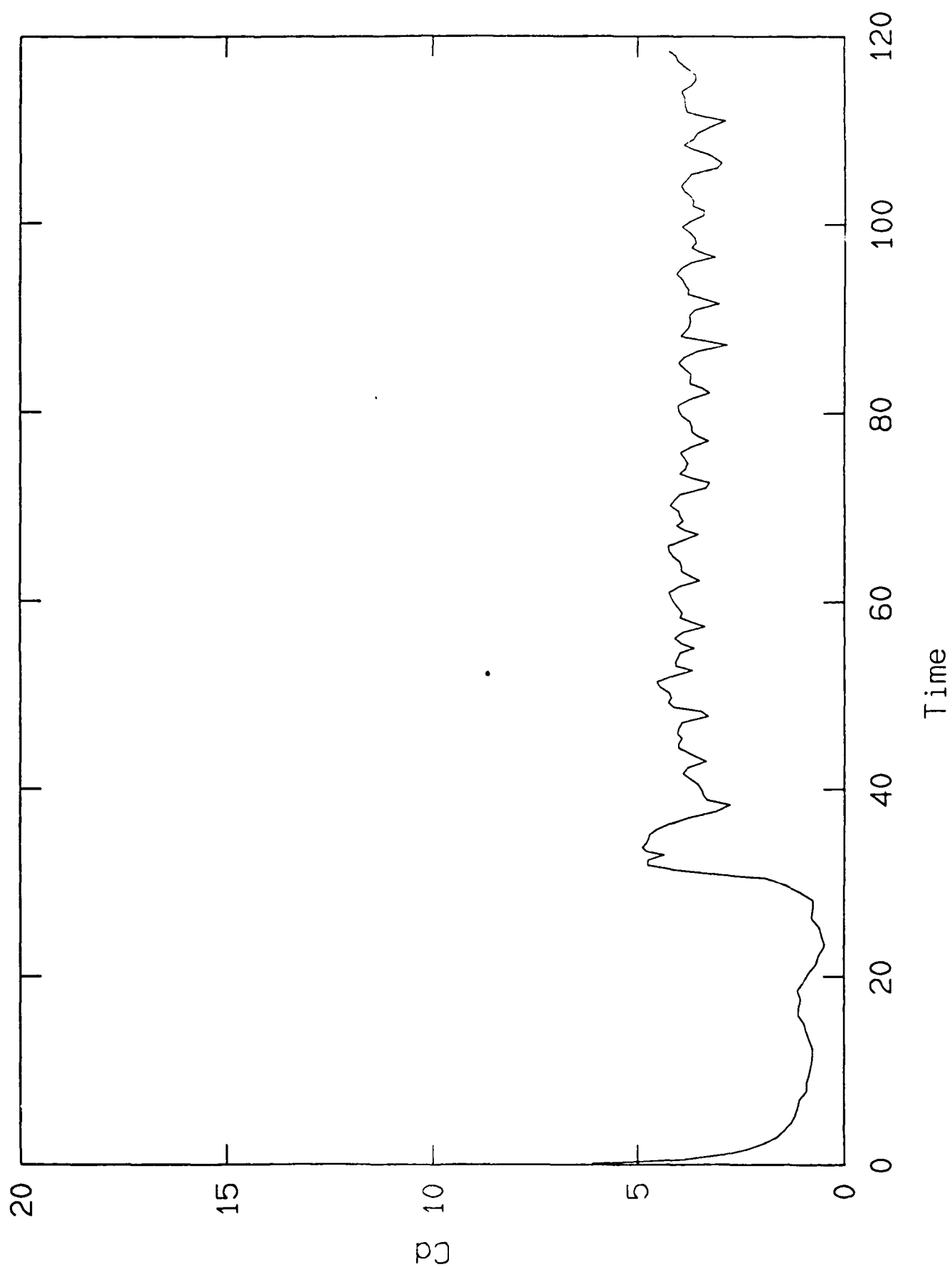


Figure 8. C_D vs x/c ; Stationary Plate

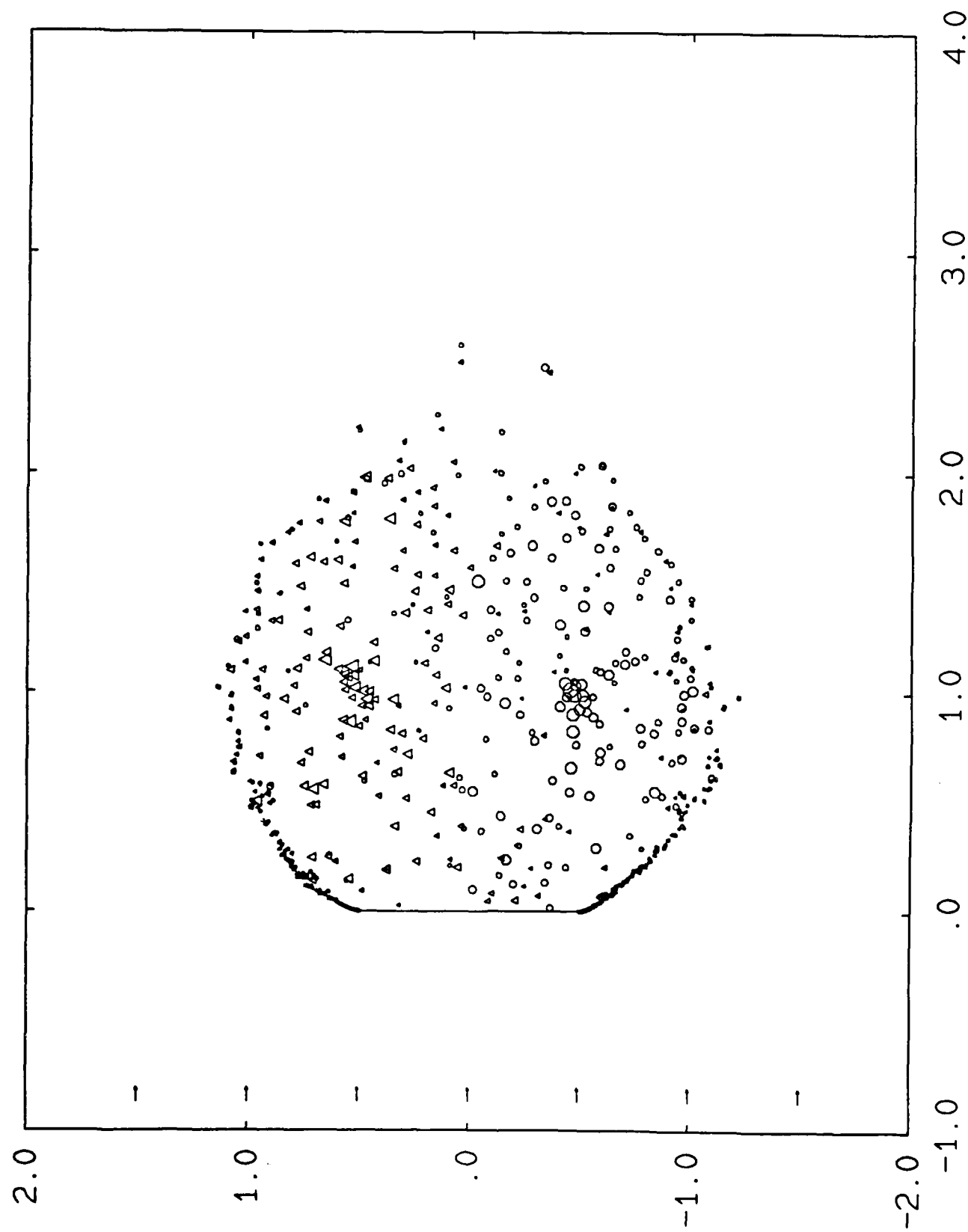


Figure 9. Time = 7.3 ($x/c = 7.3$)

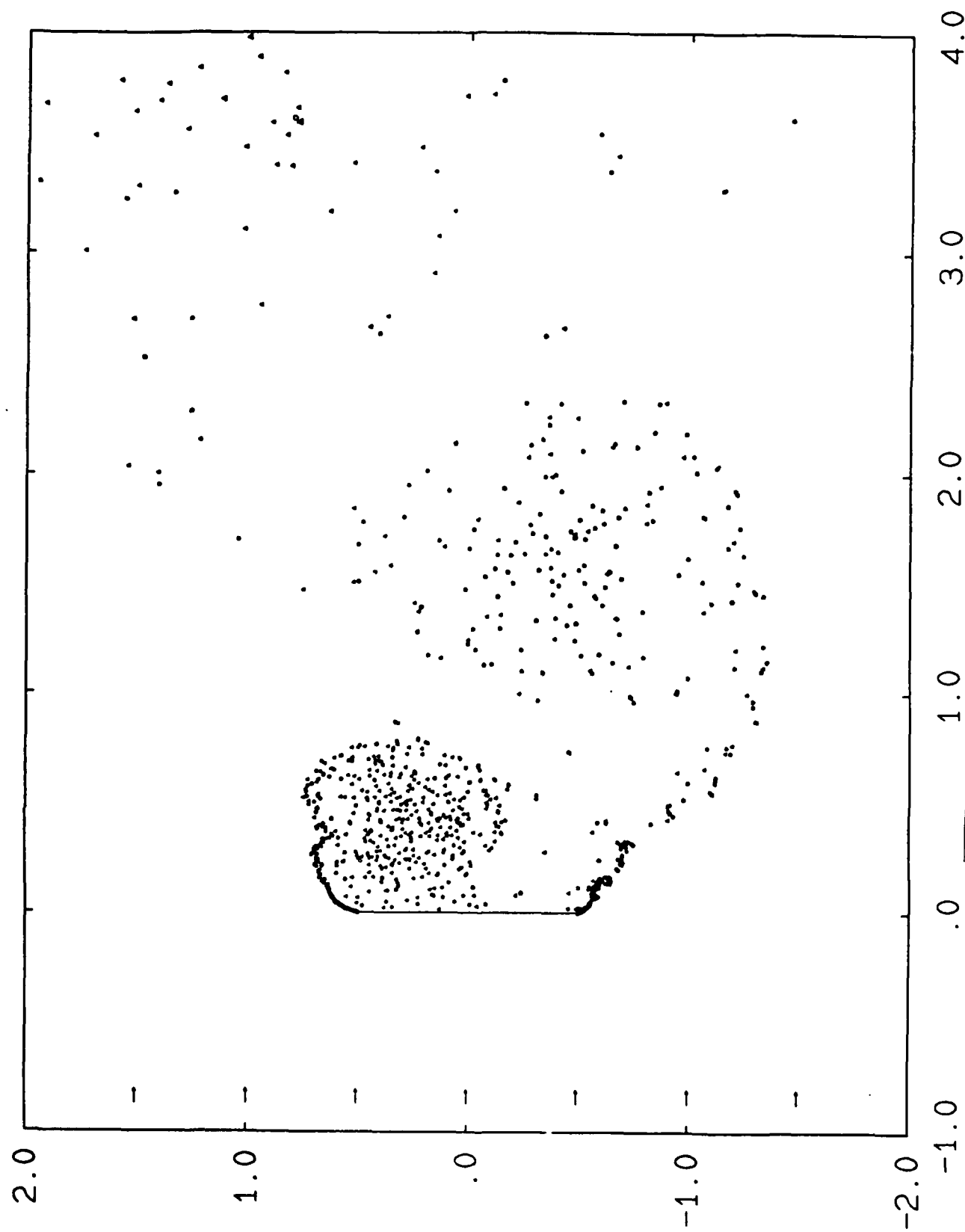


Figure 10. Wake at Time = 100 ($x/c = 100$)

Max tip speed : 2, Max Amplitude : 36.5 deg, Period : 1

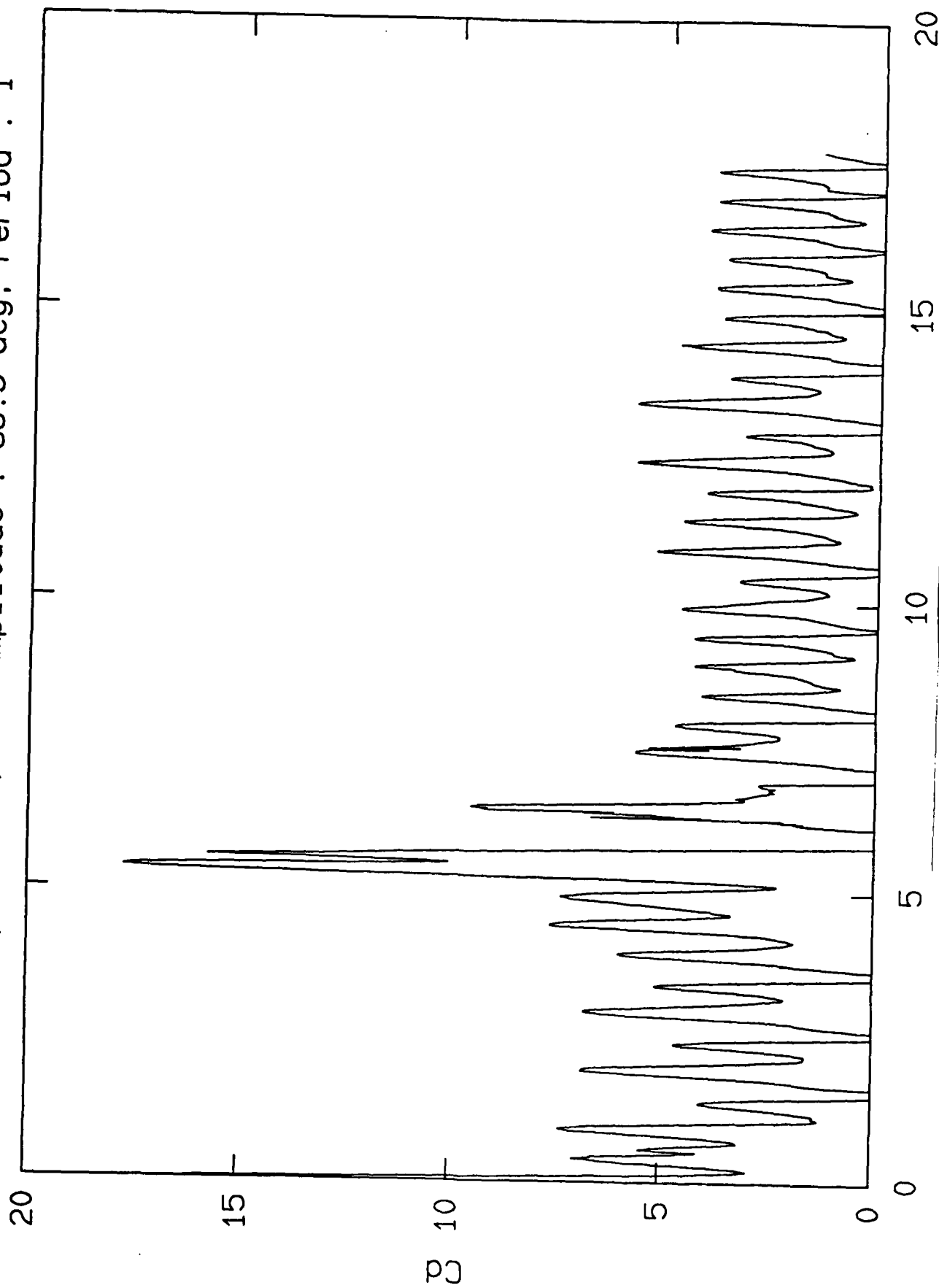


Figure 11. C_D vs x/c ; Pitching Plate

Max tip speed : 2, Max amplitude : 36.5 deg, Period : 1

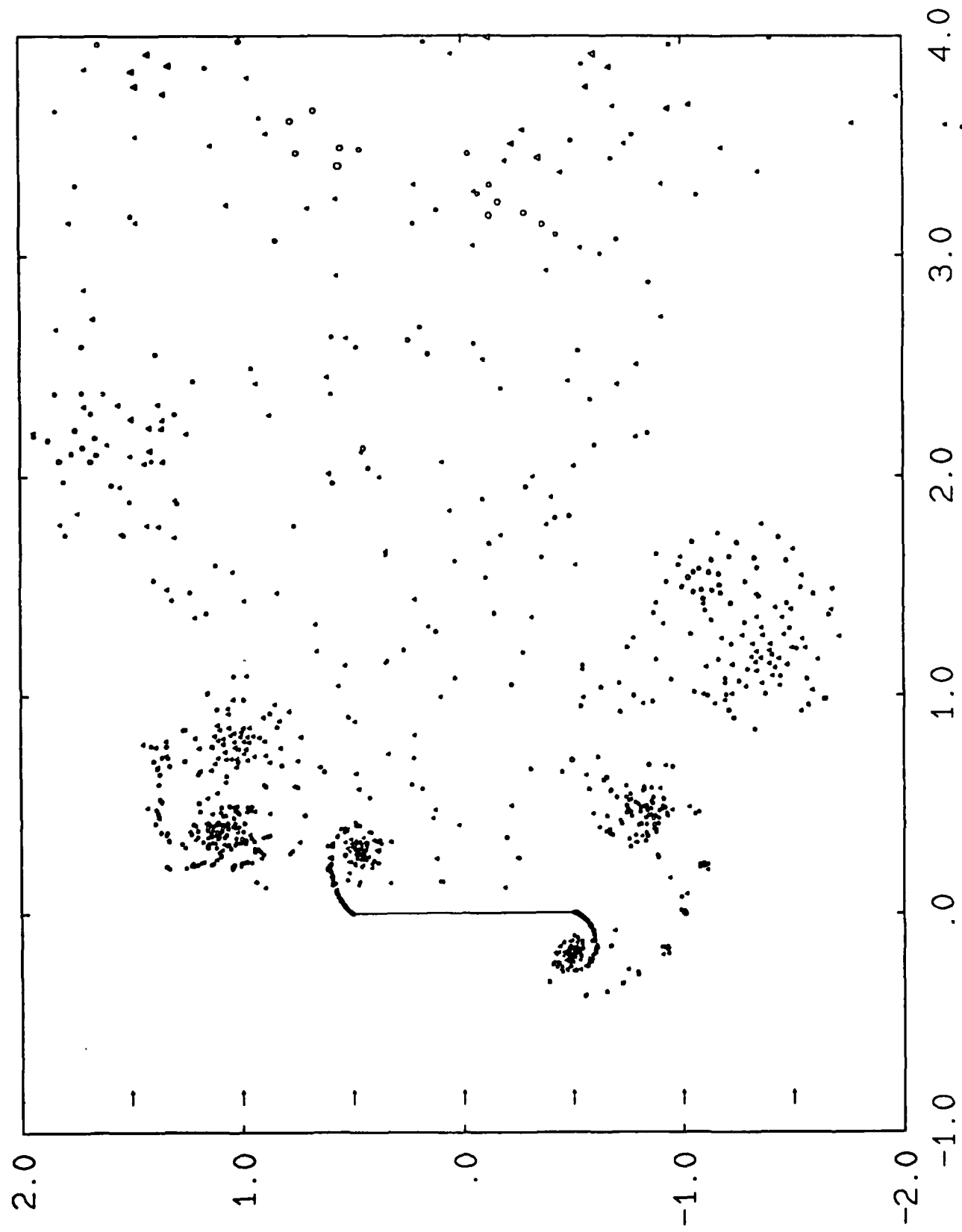


Figure 12. Vortex Clouds; Pitching Plate

Related Publications

1. K. Chua, A. Leonard, F. Pepin and G. Winckelmans 1988 "Robust Vortex Methods for Three-dimensional Incompressible Flows," In: Recent Developments in Computational Fluid Dynamics (T.E. Tezduyar and T.J.R. Hughes, eds.), Presented at Meeting of American Soc. of Mech. Engrs., Chicago, Illinois, Nov. 27-Dec. 2.
2. P.T. Tokumaru and P.E. Dimotakis, "Rotary Oscillation Control of a Cylinder Wake," AIAA 2nd Shear Flow Control Conference, March 13-16, 1989, Tempe, Arizona.
3. M. Gharib and C. Willert 1988 "Particle Tracing: Revisited," Proc. First National Fluid Dynamics Congress, Cincinnati, Ohio, pp. 1935-1943.
4. A. Leonard and K. Chua 1988 "Three-dimensional Interactions of Vortex Tubes," Proc. Symp. on Advances in Turbulence, Los Alamos, New Mexico, May 16-20.
5. C.H.K. Williamson and A. Roshko 1988 "Vortex Formation in the Wake of an Oscillating Cylinder," Journal of Fluids and Structures 2, 355-381.

PERSONNEL

Faculty

P. Dimotakis
A. Leonard
A. Roshko
J. Doyle

Visiting Faculty

M. Gharib (UCSD)

Sr. Research Fellow

C.H.K. Williamson

Graduate Students

G. Cardell
K. Chua
P. Koumoutsakos
D. Lisoski
P. Tokumaru

Other Interactions

A. Roshko was Senior Visiting Fellow at the Stanford/Ames Center for Turbulence Research during April and May of this year.

Capt. John Wissler of the U.S. Air Force Academy is enrolled as a graduate student in Aeronautics here. He will soon be deciding on a research problem in some area of unsteady flow and its control.

Discussions and other communication has continued with Dr. M. Koochesfahani, presently Assistant Professor, Michigan State University.